A Variable Sampling Interval Side-sensitive Synthetic Coefficient of Variation Chart

S.L. Lim^{1*}, W.C. Yeong^{2,3}, Michael B.C. Khoo⁴, N.R. Mataka¹ and P.S. Ng⁵

¹School of Accounting and Finance, Faculty of Business & Law, Taylor's University, 1, Jalan Taylors, Subang Jaya, 47500 Selangor Malaysia

²Centre for Big Data and Blockchain Technologies, CoE for Advanced Cloud

³Faculty of Computing & Informatics, Multimedia University, Persiaran Multimedia, 63100 Cyberjaya, Selangor,

Malaysia

⁴School of Mathematical Sciences, Universiti Sains Malaysia, 11800 Penang, Malaysia

⁵Department of Physical and Mathematical Science, Faculty of Science, Universiti Tunku Abdul Rahman, 31900 Perak,

Malaysia

The side-sensitive synthetic chart has been shown to effectively detect changes in the coefficient of variation (γ) , though its reliance on fixed sampling intervals may reduce its efficiency when compared to adaptive strategies. This paper aims to improve the chart by incorporating the variable sampling interval (VSI) feature that varies the sampling interval based on the performance of the plotting statistic of the previous sample. Formulae for the average and standard deviation of the time to signal (ATS and SDTS) of the proposed chart are derived, and procedures that optimise the chart's performance are given. Numerical comparisons reveal that the VSI feature enhances the performance of the side-sensitive synthetic γ chart by resulting in smaller out-of-control ATS values. Furthermore, an actual example is given to illustrate the effectiveness of the proposed chart in detecting out-of-control conditions in practical settings.

Keywords: Average time to signal coefficient of variation; side-sensitive; synthetic chart; variable sampling interval

I. INTRODUCTION

Control charts can detect changes in certain statistical parameters which indicates the presence of assignable causes that needs to be detected and removed as they frequently result in a deterioration in the quality of the products manufactured or the services provided.

Numerous control charts have been proposed to reduce the number of samples required to detect the out-of-control condition. One such chart is the synthetic-type chart that was first proposed by Wu and Spedding (2000) for monitoring the process mean (μ) . This concept was later extended by Wu and Spedding (2001) for monitoring the fraction non-conforming, by Calzada and Scariano (2013) for the

for the process variability, and by Celano and Castagliola (2016) for monitoring the ratio between normal variables. This chart differs from other charts by requiring two successive samples to fall outside the control limits before signalling an out-of-control condition. For conventional charts that signals an out-of-control condition right after a sample falls outside the limits, narrow control limits will result in higher number false alarms, as it is more likely for an in-control sample to fall outside the limits; however, increasing the width of the control limits will result in a delay in the detection of the out-of-control assignable cause(s), as it is more likely for out-of-control samples to fall within the

limits. By requiring two successive samples to fall outside the

coefficient of variation (γ) , by Rajmanya and Ghute (2014)

^{*}Corresponding author's e-mail: sokli.lim@taylors.edu.my

control limits before signalling an out-of-control condition, the shortcomings in conventional charts can be reduced where narrower limits can be adopted to reduce the time required to detect the out-of-control assignable cause(s), without increasing the number of false alarms.

To further improve the chart's sensitivity, Yeong *et al.* (2021) proposed the side-sensitive version of the synthetic chart by Calzada and Scariano (2013), where successive samples falling outside the control limits need to be on the same side of the limits. This allows for stricter control limits without increasing its' false alarm rate, thereby improving its' performance.

The chart by Yeong $et\ al.\ (2021)$ adopts fixed sampling intervals (d), where sampling is done at regular intervals. This approach is not optimal as unnecessarily frequent sampling may be conducted even with little evidence of an out-of-control process, thereby increasing its' sampling cost; on the other hand, sampling frequency is not increased when such evidence is present, resulting in a delay in the detection of the assignable cause(s). Hence, a better approach would be to vary d based on previous sample information, that is, by adopting a variable sampling interval (VSI) approach.

Castagliola *et al.* (2013) was the first to adopt the VSI approach to monitor γ , which was extended by Amdouni *et al.* (2017) for short production runs and Nguyen et al. (2019) for the multivariate γ . The VSI approach was also incorporated into the exponentially weighted moving average (EWMA) chart, where Yeong *et al.* (2017) monitored the univariate γ while Nguyen *et al.* (2021) and Ayyoub *et al.* (2022) monitored the multivariate γ . In addition, the VSI feature was incorporated into the cumulative sum (CUSUM) chart (Tran & Heuchenne, 2021), and the run sum chart (Yeong *et al.*, 2022). In all these charts, the VSI approach results in better performance.

This paper proposes the VSI side-sensitive synthetic γ chart, which has yet to be investigated in the literature. The proposed chart will be illustrated in the following section and subsequently evaluated through numerical analysis in Section III. An analysis of the charting parameters that affects the chart's performance is presented in this section as well. Subsequently, a comparison is made with the fixed sampling interval counterpart to highlight the appealing feature of adopting the VSI scheme. The VSI side-sensitive γ chart is

then applied to an actual manufacturing example in Section IV. Lastly, the concluding remarks are given.

II. VSI SIDE-SENSITIVE SYNTHETIC γ CHART

Let $\{X_1, X_2, ..., X_n\}$ be a sample of size n where X_i is assumed to be independent and identically distributed normal variables with a mean of μ and a standard deviation of σ . The sample γ $(\hat{\gamma})$ is obtained as:

$$\hat{\gamma} = \frac{S}{\overline{X}} \,, \tag{1}$$

where \overline{X} and S are the sample mean and standard deviation, respectively, with

 $\overline{X} = \frac{\sum_{i=1}^{n} X_i}{n},$ (2)

and

$$S = \sqrt{\frac{\sum_{i=1}^{n} (X_i - \overline{X})^2}{n-1}} .$$
 (3)

The $\hat{\gamma}$ is compared against the upper and lower control limits (*UCL* and *LCL*). If $LCL < \hat{\gamma} < UCL$, then this sample is conforming. The first $\hat{\gamma}$ that falls outside the limits is denoted as non-conforming, and the number of conforming samples until its' occurrence is called the conforming run length (*CRL*). For instance, by referring to Figure 1, $\hat{\gamma}_2$ falls above *UCL*, hence $CRL_1 = 2$. An out-of-control signal is generated if $CRL \le L$, where L is pre-determined.

For the second $\hat{\gamma}$ onwards that is outside the limits, whether the sample is conforming or not depends on the most recent non-conforming sample. If the most recent non-conforming sample is above the *UCL* (below the *LCL*), then only samples above the *UCL* (below the *LCL*) are considered as non-conforming samples. For example, by referring to Figure 1, although Sample 5 is below the *LCL*, the sample is conforming as the most recent non-conforming sample (Sample 2) is above the *UCL*. Only Sample 7 is non-conforming. Hence, $CRL_2 = 5$. Similarly, the CRL will be compared with L, producing an out-of-control signal when $CRL \leq L$.

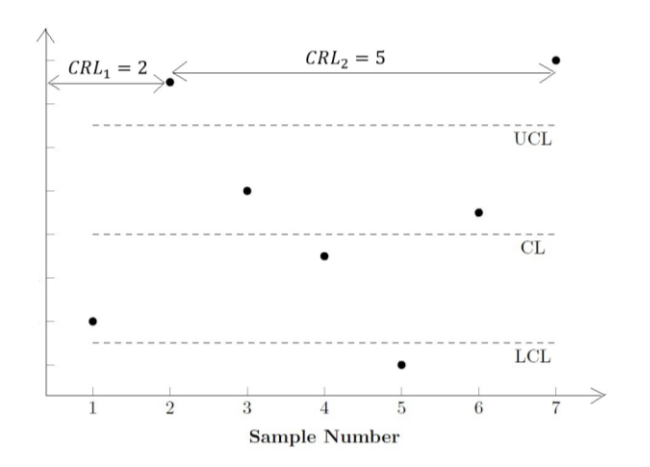


Figure 1. Side-sensitive synthetic- γ chart

The *LCL* and *UCL* are computed as (Calzada & Scariano, 2013):

$$LCL = \mu_0(\hat{\gamma}) - K\sigma_0(\hat{\gamma}), \tag{4}$$

and

$$UCL = \mu_0(\hat{\gamma}) + K\sigma_0(\hat{\gamma}), \tag{5}$$

where $\mu_0(\hat{\gamma})$ and $\sigma_0(\hat{\gamma})$ can be approximated as (Reh & Scheffler, 1996):

$$\mu_0(\hat{\gamma}) \approx \gamma_0 \left[1 + \frac{1}{n} \left(\gamma_0^2 - \frac{1}{4} \right) + \frac{1}{n^2} \left(3\gamma_0^4 - \frac{\gamma_0^2}{4} - \frac{7}{32} \right) + \frac{1}{n^3} \left(15\gamma_0^6 - \frac{3\gamma_0^4}{4} - \frac{7\gamma_0^2}{32} - \frac{19}{128} \right) \right]$$

(6)

and

$$\sigma_{0}(\hat{\gamma}) \approx \gamma_{0} \sqrt{\frac{1}{n} \left(\gamma_{0}^{2} + \frac{1}{2}\right) + \frac{1}{n^{2}} \left(8\gamma_{0}^{4} + \gamma_{0}^{2} + \frac{3}{8}\right) + \frac{1}{n^{3}} \left(69\gamma_{0}^{6} + \frac{7\gamma_{0}^{4}}{2} + \frac{3\gamma_{0}^{2}}{4} + \frac{3}{16}\right)}.$$
(7)

To determine (L,K), a wide range of L values will be considered, for example $L \in \{2,3,...,100\}$. For each of these L values, numerical methods, for example simplex search algorithms, will be adopted to obtain the value of K that minimises the time to detect assignable cause(s), while at the same time satisfying constraints in the number of false alarms. Subsequently, the (L,K) combination which shows the quickest detection of the out-of-control assignable cause(s) will be adopted.

In the side-sensitive synthetic γ chart by Yeong *et al.* (2021), sampling is done at regular intervals, i.e., the same d is adopted throughout the monitoring process. This can lead to inefficient use of sampling resources as the fixed sampling strategy does not consider the performance of the current plotting statistic $\hat{\gamma}$ when determining the sampling frequency for the next sample. This limitation serves as a motivation for this paper to incorporate the VSI feature.

Figure 2 depicts the operation for the VSI side-sensitive synthetic γ chart, where the region between LCL and UCL is separated into the central (o_c) and warning (o_w) conforming regions. If $\hat{\gamma}$ falls in o_c , the next sample is collected after a long interval (d_2) , whereas the next sample is collected after a short interval (d_1) if $\hat{\gamma}$ falls in o_w or the non-conforming regions. The conforming region is separated into o_c and o_w through the LWL and UWL as shown in Figure 2. The LWL and UWL can be obtained from Equations (4) and (5) by replacing K with the warning limit coefficient (W), where W < K.

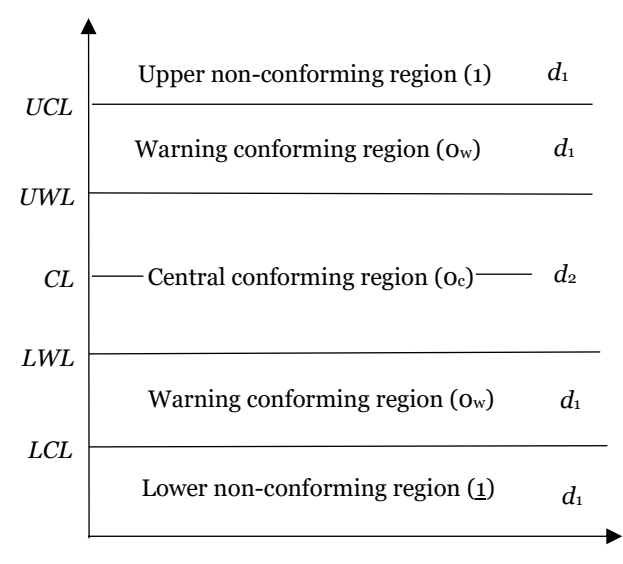


Figure 2. The operation of the VSI side-sensitive synthetic γ chart

The performance of the VSI side-sensitive synthetic γ chart is evaluated through the average and standard deviation of the time to signal (ATS and SDTS). Saccucci et al. (1992) developed a Markov chain approach for the ATS and SDTS by forming different in-control transient states and a single out-of-control absorbing state. Subsequently, the ATS and SDTS are obtained through the average and standard deviation of

the number of transitions until the Markov chain reaches the absorbing state, as follows:

$$ATS = \mathbf{q}^{T} (\mathbf{Q} - \mathbf{I}) \mathbf{d}$$
 (8)

and

$$SDTS = \sqrt{\mathbf{q}^{T} \mathbf{Q} \mathbf{B} (2\mathbf{Q} - \mathbf{I}) \mathbf{d} - (\mathbf{q}^{T} \mathbf{Q} \mathbf{d})^{2}},$$
(9)

where the notations are described in Table 1. Equations (8) and (9) are widely adopted in various charts with the VSI feature, for example by Nguyen *et al.* (2021), Xie *et al.* (2022), Yeong *et al.* (2024), Bai *et al.* (2024), Adsiz and Aytacoglu (2024), Hu *et al.* (2024), and many others.

Table 1. Notations in Equations (8) and (9)

Notations	Description		
q	Initial probability vector		
Q	Transition probability		
	matrix of the in-control		
	states		
I	Identity matrix		
d	Vector of sampling		
	intervals associated with		
	its' respective states		
В	Diagonal matrix with the i th		
	diagonal being equivalent		
	to the i^{th} element of d		

To apply Equations (8) and (9) on the proposed chart, the states of the Markov chain are defined based on L consecutive $\hat{\gamma}$, as follows:

State 1: <u>1</u>00... 00c

State 2: <u>1</u>00... 00w

State 3: 010... 00c

State 4: 010... 00w

:

State 2*L*-3: 000... <u>1</u>0c

State 2*L*-2: 000... <u>1</u>0w

State 2*L*-1: 000...0<u>1</u>

State 2L: 000... 00c

State 2L+1: 000... 00w

State 2*L*+2: 00...001

State 2L+3: 000...10c

State 2L+4: 000... 10w

State 4*L*-1: 100... 00c

State 4*L*: 100... 00_w

State 4L+1: Signalling (absorbing) state

For example, by letting $\hat{\gamma}_i$ denote the $\hat{\gamma}$ of the i^{th} sample, State 1 (100... ooc) is the state where $\,\hat{\gamma}_1$ falls in region 1, $\,\hat{\gamma}_2$ to $\hat{\gamma}_{L-1}$ are conforming samples, while $\hat{\gamma}_L$ falls in region oc. Note that the sampling interval to be adopted only depends on the region for its' most recent sample, hence only the specific conforming region for $\,\hat{\gamma}_{\scriptscriptstyle L}\,$ needs to be specified, while for $\hat{\gamma}_{_{\! 1}}$ to $\hat{\gamma}_{_{L-1}}$, as long as they fall in the conforming region, they are generalized as region o. The differing positions for 1 and 1 among the different states have an impact on the CRL following the occurrence of $\hat{\gamma}_{{\scriptscriptstyle L}+1}$, which impacts the probability of transitioning to State 4L+1, the out-of-control absorbing state which occurs if $CRL \le L$. For example, if its' Markov chain is currently in State 1, and $\hat{\gamma}_{L+1}$ is in region 1, then the CRL = L and the Markov chain transitions to State 4*L*+1. If $\hat{\gamma}_{\scriptscriptstyle{L+1}}$ falls in the other regions, then the Markov chain will transition to the other in-control states since CRL > L.

The **Q** matrix in Equations (8) and (9) can be obtained for the proposed chart from the transition probabilities among States 1 to 4L, i.e. the in-control states. The matrix **Q** is obtained by combining Tables 2a to 2c, where Table 2a shows the transition probabilities to States 1 to 2L-2, Table 2b shows the probabilities to States 2L-1 to 2L+4 while Table 2c shows the probabilities to States 2L-5 to 4L.

Table 2a. Transition probabilities to States 1 to 2L-2

States	1	2	3	4	5	6	•••	2L-3	2L-2
1									
2									
3	A	В							
4	A	В							
5			A	В					
6			A	В					
:									
2L-1								A	В
2L									
2L + 1									

2L+2					
2L+3					
2L+4					
:					
4 <i>L</i> – 1					
4L					

Table 2b. Transition probabilities to States 2L-1 to 2L+4

Table 201 Transition probabilities to States 22 T to 22 1 7						
States	2L-1	2L	2L + 1	2L+2	2L+3	2L + 4
1		A	В	С		
2		A	В	С		
3				С		
4				С		
5				С		
6				С		
:						
2L-1				С		
2L	D	A	В	С		
2L+1	D	A	В	С		
2L+2	D				A	В
2L+3	D					
2L+4	D					
:						
4 <i>L</i> – 1	D	A	В			
4L	D	A	В			

Table 2c. Transition probabilities to States 2L+5 to 4L

States	2L+5	2L+6	•••	4L-1	4L
1					
2					
3					
4					
5					
6					
:					
2L-1					
2L					
2L+1					
2L+2					
2L+3	A	В			

2 <i>L</i> + 4	A	В		
÷				
4 <i>L</i> – 1				
4L				

The empty entries in Tables 2a to 2c are 0, while A, B, C and D are the probabilities $\hat{\gamma}$ will fall in regions O_c , O_w , 1 and $\underline{1}$, respectively. To illustrate how the transition probabilities are obtained, we refer to Table 2a on the transition from States 3 to 1. The transition probability is A since if the current state is State 3, i.e. $O\underline{1}O$... OO_c , and the next $\hat{\gamma}$ falls in region O_c , which happens with a probability of A, then the state will transition to $\underline{1}OO$... OO_c which is State 1. Thus, $p_{31} = A$. The following shows how A, B, C and D are obtained:

$$A = F_{\hat{r}}(UWL) - F_{\hat{r}}(LWL) \tag{10}$$

$$B = F_{\hat{\tau}}(LWL) - F_{\hat{\tau}}(LCL) + F_{\hat{\tau}}(UCL) - F_{\hat{\tau}}(UWL)$$
 (11)

$$C = 1 - F_{\hat{x}}(UCL) \tag{12}$$

and

$$D = F_{\hat{\gamma}}(LCL), \tag{13}$$

where $F_{\hat{\gamma}}(.)$ is the cumulative distribution function (cdf) of $\hat{\gamma}$ which is computed as (Castagliola et al., 2011):

$$F_{\hat{\gamma}}(x) = 1 - F_{t}\left(\frac{\sqrt{n}}{x}\right),\tag{14}$$

where $F_{\iota}(.)$ is the cdf of the non-central t distribution with (n-1) degrees of freedom and non-centrality parameter

$$\frac{\sqrt{n}}{\gamma}$$
.

Next, to obtain ${\bf q}$, we assume that the process will start at State 2L+2, for a quick detection of early positive shifts. Hence, the $(2L+2)^{\rm th}$ element of ${\bf q}$ is one, with the other elements being 0. Positive shifts in γ , i.e. where there is an increase in the in-control γ (γ_0) , is more critical to a process as it shows increased variability when the ratio of σ over μ has increased. Hence, it is important that positive shifts can be detected quickly.

To obtain \mathbf{d} , the elements associated with the states where $\hat{\gamma}_L$ falls in region o_c , for example States 1, 3, ..., will be assigned d_2 , while the other elements are assigned d_1 .

By defining how \mathbf{Q} , \mathbf{q} and \mathbf{d} are obtained, the ATS and SDTS can be obtained from Equations (8) and (9). The incontrol ATS and SDTS (ATS_0 and $SDTS_0$) lets $\gamma=\gamma_0$ in Equations (10) to (13), while the out-of-control ATS and SDTS (ATS_1 and $SDTS_1$) lets $\gamma=\tau\gamma_0$ in Equations (10) to (13), where τ is the shift in γ_0 . Note that the ATS_0 and $SDTS_0$ evaluate the average and the standard deviation for the time until a chart signals a false alarm, i.e. where the chart gives an out-of-control signal but the process is actually in-control, whereas its' ATS_1 and $SDTS_1$ evaluate the average and the standard deviation for the time until the out-of-control assignable cause(s) is detected.

In the next section, the chart's performance will be analysed through numerical examples and compared with its' counterpart without the VSI feature.

III. NUMERICAL ANALYSIS

The performance of the VSI side-sensitive synthetic chart will be evaluated through numerical examples. We consider the parameters of $\tau \in \{1.1,1.2,1.5,2.0,2.5\}$, $n \in \{5,7,10,15\}$, $\gamma_0 \in \{0.05,0.10,0.15,0.20\}$ and $(d_1,d_2) \in \{(0.1,1.5),(0.1,1.9),(0.1,4.0)\}$, which are consistent with those

The following procedure is adopted to obtain the optimal (L,W,K), together with its' corresponding $(ATS_1,SDTS_1)$:

1. Specify the values for τ , n, γ_0 , d_1 and d_2 .

previously adopted by Castagliola et al. (2013).

- 2. Initialise L = 2.
- 3. Numerical methods, for example simplex search algorithms, are applied to obtain the (W,K) combination that minimises the ATS_1 , while satisfying the constraint $ATS_0 = 370.4$. The ATS is computed from Equation (8).
- 4. Increase L by 1.
- 5. Repeat Steps 3 and 4 until L=100.
- 6. Among all the combinations of (L,W,K), the optimal (L,W,K) is the combination with the smallest ATS_1 . With the optimal (L,W,K), the $SDTS_1$ is computed from Equation (9). Tables 3, 4, 5 and 6 show the optimal (L,W,K) and the corresponding ATS_1 and $SDTS_1$ for

 $\gamma_0 = 0.05$, $\gamma_0 = 0.10$, $\gamma_0 = 0.15$ and $\gamma_0 = 0.20$, respectively. For instance, from Table 3, for $\gamma_0 = 0.05$, n = 5, $\tau = 1.1$ and $(d_1, d_2) = (0.1, 1.5)$, the optimal (L, W, K) = (42, 0.93, 2.65), which results in $(ATS_1, SDTS_1) = (60.88, 80.96)$.

Table 3. Optimal (L, W, K) and the corresponding $(ATS_1, SDTS_1)$ for $\gamma_0 = 0.05$, $n \in \{5, 7, 10, 15\}$ and $(d_1, d_2) \in \{(0.1, 1.5), (0.1, 1.9), (0.1, 4.0)\}$

τ		n = 5	,
	(0.1,1.5)	(0.1,1.9)	(0.1,4.0)
1.1	42, 0.93, 2.65	42, 0.69, 2.65	42, 0.30, 2.65
	60.88, 80.96	60.70, 80.85	60.52, 81.34
1.2	23, 0.93, 2.52	23, 0.69, 2.52	23, 0.30, 2.52
	18.30, 24.43	18.14, 24.36	17.99, 24.85
1.5	8, 0.93, 2.28	8, 0.69, 2.28	8, 0.30, 2.28
	2.45, 3.54	2.38, 3.57	2.32, 4.05
2.0	4, 0.93, 2.11	4, 0.69, 2.11	4, 0.30, 2.11
	0.49, 1.00	0.47, 1.05	0.44, 1.34
2.5	3, 0.93, 2.05	3, 0.69, 2.05	3, 0.30, 2.05
	0.18, 0.55	0.17, 0.58	0.16, 0.77
τ		n = 7	
1.1	37, 0.93, 2.57	37, 0.68, 2.57	37, 0.30, 2.57
	48.39, 64.40	48.16, 64.24	47.95, 64.66
1.2	19, 0.93, 2.43	19, 0.68, 2.43	19, 0.30, 2.43
	12.91, 17.27	12.17, 17.17	12.63, 17.63
1.5	7, 0.93, 2.22	7, 0.68, 2.22	7, 0.30, 2.22
	1.44, 2.22	1.39, 2.25	1.33, 2.67
2.0	3, 0.93, 2.03	3, 0.68, 2.03	3, 0.30, 2.03
	0.23, 0.62	0.21, 0.65	0.20, 0.85
2.5	3, 0.93, 2.03	3, 0.68, 2.03	3, 0.30, 2.03
	0.07, 0.31	0.06, 0.32	0.06, 0.43
τ		n = 10	
1.1	35, 0.93, 2.52	35, 0.68, 2.52	35, 0.30, 2.52
	37.61, 49.96	37.34, 49.75	37.09, 50.12
1.2	16, 0.93, 2.37	16, 0.68, 2.37	16, 0.30, 2.37
	8.77, 11.77	8.59, 11.67	8.42, 12.11
1.5	5, 0.93, 2.14	5, 0.68, 2.14	5, 0.30, 2.14
	0.78, 1.39	0.73, 1.41	0.69, 1.74
2.0	3, 0.93, 2.03	3, 0.68, 2.03	3, 0.30, 2.03
	0.09, 0.35	0.08, 0.36	0.07, 0.47
2.5	2, 0.93, 1.94	2, 0.68, 1.94	2, 0.30, 1.94
	0.02, 0.15	0.02, 0.15	0.01, 0.20
τ		n = 15	1
	1		

1.1	31, 0.92, 2.48	31, 0.68, 2.48	31, 0.30, 2.48
	27.53, 36.51	27.24, 36.26	26.95, 36.58
1.2	13, 0.92, 2.32	13, 0.68, 2.32	13, 0.30, 2.32
	5.39, 7.31	5.23, 7.23	5.06, 7.65
1.5	4, 0.92, 2.09	4, 0.68, 2.09	4, 0.30, 2.09
	0.34, 0.78	0.31, 0.80	0.29, 1.02
2.0	2, 0.92, 1.94	2, 0.68, 1.94	2, 0.30, 1.94
	0.02, 0.16	0.02, 0.16	0.02, 0.21
2.5	2, 0.92, 1.94	2, 0.68, 1.94	2, 0.30, 1.94
	0.002, 0.05	0.002,0.05	0.001, 0.06

Table 4. Optimal (L,W,K) and the corresponding $(ATS_1,SDTS_1)$ for $\gamma_0=0.10,\ n\in\{5,7,10,15\}$ and $(d_1,d_2)\in\{(0.1,1.5),(0.1,1.9),(0.1,4.0)\}$

_	n = 5				
τ	(0.1,1.5)	(0.1,1.9)	(0.1,4.0)		
1.1	42, 0.93, 2.67	42, 0.69, 2.67	42, 0.30, 2.67		
	61.34, 81.58	61.17, 81.48	61.02, 81.99		
1.2	23, 0.93, 2.54	23, 0.69, 2.54	23, 0.30, 2.54		
	18.52, 24.74	18.37, 24.67	18.23, 25.17		
1.5	8, 0.93, 2.29	8, 0.69, 2.29	8, 0.30, 2.29		
	2.50, 3.61	2.43, 3.64	2.37, 4.12		
2.0	4, 0.93, 2.12	4, 0.69, 2.12	4, 0.30, 2.12		
	0.50, 1.02	0.48, 1.07	0.46, 1.37		
2.5	3, 0.93, 2.05	3, 0.69, 2.05	3, 0.30, 2.05		
	0.19, 0.56	0.18, 0.59	0.17, 0.79		
τ	n = 7				
1.1	36, 0.93, 2.58	36, 0.68, 2.58	36, 0.30, 2.58		
	48.83, 65.01	48.61, 64.86	48.42, 65.31		
1.2	19, 0.93, 2.44	19, 0.68, 2.44	19, 0.30, 2.44		
	13.08, 17.52	12.91, 17.43	12.75, 17.89		
1.5	7, 0.93, 2.23	7, 0.68, 2.23	7, 0.30, 2.23		
	1.48, 2.27	1.42, 2.30	1.36, 2.72		
2.0	3, 0.93, 2.04	3, 0.68, 2.04	3, 0.30, 2.04		
	0.24, 0.64	0.22, 0.66	0.21, 0.87		
2.5	3, 0.93, 2.04	3, 0.68, 2.04	3, 0.30, 2.04		
	0.07, 0.32	0.07, 0.34	0.06, 0.45		
τ		n = 10			
1.1	35, 0.93, 2.53	35, 0.68, 2.53	35, 0.30, 2.53		
	37.90, 50.36	37.64, 50.16	37.41, 50.55		
1.2	16, 0.93, 2.38	16, 0.68, 2.38	16, 0.30, 2.38		
	8.90, 11.94	8.72, 11.85	8.56, 12.29		
1.5	5, 0.93, 2.14	5, 0.68, 2.14	5, 0.30, 2.14		
	0.80, 1.42	0.76, 1.45	0.71, 1.77		

2.0	3, 0.93, 2.03	3, 0.68, 2.03	3, 0.30, 2.03
	0.09, 0.36	0.08, 0.37	0.07, 0.49
2.5	2, 0.93, 1.94	2, 0.68, 1.94	2, 0.30, 1.94
	0.02, 0.16	0.02, 0.16	0.02, 0.21
τ		n = 15	
1.1	31, 0.92, 2.49	31, 0.68, 2.49	31, 0.30, 2.49
	27.73, 36.78	27.44, 36.54	27.17, 36.88
1.2	13, 0.92, 2.32	13, 0.68, 2.32	13, 0.30, 2.32
	5.48, 7.44	5.32, 7.35	5.16, 7.78
1.5	4, 0.92, 2.09	4, 0.68, 2.09	4, 0.30, 2.09
	0.36, 0.81	0.33, 0.82	0.30, 1.04
2.0	2, 0.92, 1.94	2, 0.68, 1.94	2, 0.30, 1.94
	0.02, 0.17	0.02, 0.17	0.02, 0.22
2.5	2, 0.92, 1.94	2, 0.68, 1.94	2, 0.30, 1.94
	0.002, 0.05	0.002,0.05	0.002, 0.06

Table 5. Optimal (L, W, K) and the corresponding $(ATS_1, SDTS_1)$ for $\gamma_0 = 0.15$, $n \in \{5, 7, 10, 15\}$ and $(d_1, d_2) \in \{(0.1, 1.5), (0.1, 1.9), (0.1, 4.0)\}$

		n = 5	
τ	(0.1,1.5)	(0.1,1.9)	(0.1,4.0)
1.1	42, 0.93, 2.70	42, 0.68, 2.70	42, 0.30, 2.70
	62.13, 82.62	61.98, 82.56	61.86, 83.10
1.2	23, 0.93, 2.56	23, 0.68, 2.56	23, 0.30, 2.56
	18.90, 25.26	18.76, 25.20	18.63, 25.72
1.5	8, 0.93, 2.31	8, 0.68, 2.31	8, 0.30, 2.31
	2.58, 3.72	2.52, 3.76	2.46, 4.24
2.0	4, 0.93, 2.13	4, 0.68, 2.13	4, 0.30, 2.13
	0.53, 1.07	0.51, 1.11	0.49, 1.42
2.5	3, 0.93, 2.06	3, 0.68, 2.06	3, 0.30, 2.06
	0.21, 0.59	0.20, 0.62	0.19, 0.83
τ		n = 7	
1.1	36, 0.93, 2.60	36, 0.68, 2.60	36, 0.30, 2.60
	49.60, 66.06	49.41, 65.94	49.24, 66.40
1.2	19, 0.93, 2.47	19, 0.68, 2.47	19, 0.30, 2.47
	13.40, 17.95	13.24, 17.87	13.09, 18.35
1.5	7, 0.93, 2.24	7, 0.68, 2.24	7, 0.30, 2.24
	1.54, 2.35	1.48, 2.38	1.42, 2.81
2.0	3, 0.93, 2.04	3, 0.68, 2.04	3, 0.30, 2.04
	0.26, 0.67	0.24, 0.69	0.22, 0.91
2.5	3, 0.93, 2.04	3, 0.68, 2.04	3, 0.30, 2.04
	0.08, 0.34	0.07, 0.36	0.07, 0.48
τ		n = 10	
1.1	34, 0.92, 2.55	34, 0.68, 2.55	34, 0.30, 2.55

	38.44, 51.16	38.21, 50.98	37.99, 51.39		
1.2	16, 0.92, 2.39	16, 0.68, 2.39	16, 0.30, 2.39		
	9.12, 12.25	8.95, 12.16	8.79, 12.61		
1.5	5, 0.92, 2.15	5, 0.68, 2.15	5, 0.30, 2.15		
	0.84, 1.48	0.80, 1.50	0.75, 1.84		
2.0	3, 0.92, 2.04	3, 0.68, 2.04	3, 0.30, 2.04		
	0.10, 0.38	0.09, 0.40	0.08, 0.52		
2.5	2, 0.92, 1.95	2, 0.68, 1.95	2, 0.30, 1.95		
	0.02, 0.17	0.02, 0.18	0.02, 0.23		
τ	n = 15				
1.1	30, 0.92, 2.49	30, 0.68, 2.49	30, 0.30, 2.49		
	28.10, 37.35	27.83, 37.13	27.57, 37.48		
1.2	13, 0.92, 2.33	13, 0.68, 2.33	13, 0.30, 2.33		
	5.64, 7.65	5.48, 7.57	5.32, 8.00		
1.5	4, 0.92, 2.09	4, 0.68, 2.09	4, 0.30, 2.09		
	0.38, 0.84	0.35, 0.86	0.32, 1.09		
2.0	2, 0.92, 1.94	2, 0.68, 1.94	2, 0.30, 1.94		
	0.03, 0.18	0.02, 0.18	0.02, 0.23		
2.5	2, 0.92, 1.94	2, 0.68, 1.94	2, 0.30, 1.94		
	0.003, 0.06	0.002,0.06	0.002, 0.07		

Table 6. Optimal (L, W, K) and the corresponding $(ATS_1, SDTS_1)$ for $\gamma_0 = 0.20, n \in \{5, 7, 10, 15\}$ and $(d_1, d_2) \in \{(0.1, 1.5), (0.1, 1.9), (0.1, 4.0)\}$

_	n = 5		
τ	(0.1,1.5)	(0.1,1.9)	(0.1,4.0)
1.1	42, 0.92, 2.74	42, 0.68, 2.74	42, 0.30, 2.74
	63.27, 84.12	63.15, 84.10	63.06, 84.69
1.2	24, 0.92, 2.61	24, 0.68, 2.61	24, 0.30, 2.61
	19.44, 25.94	19.32, 25.91	19.21, 26.45
1.5	9, 0.92, 2.37	9, 0.68, 2.37	9, 0.30, 2.37
	2.70, 3.82	2.64, 3.87	2.58, 4.37
2.0	4, 0.92, 2.15	4, 0.68, 2.15	4, 0.30, 2.15
	0.57, 1.12	0.55, 1.17	0.52, 1.49
2.5	3, 0.92, 2.08	3, 0.68, 2.08	3, 0.30, 2.08
	0.23, 0.62	0.22, 0.66	0.21, 0.88
τ	n = 7		
1.1	36, 0.92, 2.64	36, 0.68, 2.64	36, 0.30, 2.64
	50.75, 67.60	50.58, 67.51	50.44, 68.03
1.2	19, 0.92, 2.49	19, 0.68, 2.49	19, 0.30, 2.49
	13.87, 18.60	13.72, 18.54	13.58, 19.03
1.5	7, 0.92, 2.26	7, 0.68, 2.26	7, 0.30, 2.26
	1.62, 2.46	1.57, 2.50	1.51, 2.93
2.0	3, 0.92, 2.05	3, 0.68, 2.05	3, 0.30, 2.05

	ı	I	I	
	0.28, 0.71	0.26, 0.74	0.25, 0.96	
2.5	3, 0.92, 2.05	3, 0.68, 2.05	3, 0.30, 2.05	
	0.09, 0.37	0.09, 0.39	0.08, 0.52	
τ		n = 10		
1.1	33, 0.92, 2.57	33, 0.68, 2.57	33, 0.30, 2.57	
	39.32, 52.39	39.11, 52.24	38.92, 52.69	
1.2	16, 0.92, 2.41	16, 0.68, 2.41	16, 0.30, 2.41	
	9.45, 12.71	9.29, 12.63	9.14, 13.10	
1.5	5, 0.92, 2.16	5, 0.68, 2.16	5, 0.30, 2.16	
	0.90, 1.56	0.85, 1.58	0.81, 1.93	
2.0	3, 0.92, 2.04	3, 0.68, 2.04	3, 0.30, 2.04	
	0.11, 0.41	0.10, 0.43	0.10, 0.56	
2.5	2, 0.92, 1.95	2, 0.68, 1.95	2, 0.30, 1.95	
	0.03, 0.19	0.02, 0.20	0.02, 0.26	
τ	n = 15			
1.1	30, 0.92, 2.51	30, 0.68, 2.51	30, 0.30, 2.51	
	28.70, 38.17	28.45, 37.98	28.21, 38.36	
1.2	13, 0.92, 2.34	13, 0.68, 2.34	13, 0.30, 2.34	
	5.87, 7.97	5.71, 7.89	5.56, 8.33	
1.5	4, 0.92, 2.10	4, 0.68, 2.10	4, 0.30, 2.10	
	0.41, 0.89	0.38, 0.91	0.35, 1.15	
2.0	2, 0.92, 1.95	2, 0.68, 1.95	2, 0.30, 1.95	
	0.03, 0.20	0.03, 0.20	0.02, 0.26	
2.5	2, 0.92, 1.95	2, 0.68, 1.95	2, 0.30, 1.95	
	0.004, 0.07	0.003,0.07	0.003, 0.09	

Several key observations are obtained from Tables 3 to 6. Firstly, both ATS_1 and $SDTS_1$ decrease as τ and n increase. For instance, in Table 3, $(ATS_1,SDTS_1)=(60.88,80.96)$ when $\tau=1.1$ is considered. In contrast, $(ATS_1,SDTS_1)=(0.18,0.55)$ when $\tau=2.5$ is selected. This indicates that the VSI side-sensitive synthetic γ chart becomes more effective at detecting larger shifts, as reflected by shorter detection times. Similarly, larger n enhances the detection power of the VSI side-sensitive synthetic γ chart. For example, when n increases from 5 to 15 for $\tau=1.1$ in Table 1, the ATS_1 and $SDTS_1$ decrease to 27.53 and 36.51, respectively. This shows a decrease in both the expected and variability in the time required to detect the shift, which is expected since larger τ represents a larger shifts tend to be detected more quickly.

From Tables 3 to 6, there is a marginal decrease in the ATS1 for larger gaps between d_1 and d_2 . For example, from Table

3, when n=5 and $\tau=1.1$ are considered, the $ATS_1=60.88$ for $(d_1,d_2)=(0.1,1.5)$, but decreases slightly to 60.52 when $(d_1,d_2)=(0.1,4.0)$. Furthermore, there is also a slight increase in the $(ATS_1,SDTS_1)$ for larger γ_0 . For example, when n=5, $\tau=1.1$ and $(d_1,d_2)=(0.1,1.5)$ are considered, the $(ATS_1,SDTS_1)=(60.88,80.96)$ for $\gamma_0=0.05$ (see Table 3), while the $(ATS_1,SDTS_1)=(63.27$, 84.12) for $\gamma_0=0.20$ (see Table 6).

For the choice of charting parameters, smaller L and K are adopted for larger τ and n. For instance, from Table 3, for $\gamma_0=0.05,\ n=5,\ \tau=1.1$ and $(d_1,d_2)=(0.1,1.5),\ (L,K)=(42,2.65)$, but when $\tau=2.5$, (L,K)=(3,2.05). Similarly, for $\gamma_0=0.05, n=15, \tau=1.1$ and $(d_1,d_2)=(0.1,1.5)$, smaller L and K are adopted as compared to that of n=5, with (L,K)=(31,2.48). The choice of L and K does not seem to be affected by (d_1,d_2) , where for the same γ_0 , n and τ , the same (L,K) is adopted for all three combinations of (d_1,d_2) being considered. Marginally larger K is also adopted for larger γ_0 . For example, K=2.65 for $\gamma_0=0.05, n=5$ and $\tau=1.1$ in Table 3, while K=2.74 for $\gamma_0=0.20, n=5$ and $\tau=1.1$ in Table 5.

For the choice of W, it can be observed that smaller values of W are adopted for larger gaps between d_1 and d_2 . For example, for $\gamma_0=0.05, n=5, \tau=1.1$ and $(d_1,d_2)=(0.1,1.5)$ in Table 3, W=0.93, but for the same γ_0,n and τ but with $(d_1,d_2)=(0.1,4.0)$, W becomes 0.30. W does not seem to be affected by γ_0,n and τ , with the same or similar values being adopted.

Next, the performance of the VSI side-sensitive synthetic γ chart will be compared with the side-sensitive synthetic γ chart without the VSI feature. Due to space constraints, the comparisons are made for only $\gamma_0 = 0.05$. Table 7 shows the optimal (L,K) and the corresponding ATS_1 and $SDTS_1$ for $\tau \in \{1.1,1.2,1.5,2.0,2.5\}$, $n \in \{5,7,10,15\}$ and $\gamma_0 \in \{0.05,0.10,0.15,0.20\}$. For example, for $\gamma_0 = 0.05, n = 5$

and $\tau = 1.1$, the optimal (L,K) = (42,2.65), which results in $(ATS_1,SDTS_1) = (64.74,84.69)$.

Table 7. Optimal (L,K) and the corresponding $(ATS_1,SDTS_1)$ for $\gamma_0 = 0.05$ and $n \in \{5,7,10,15\}$

τ	n = 5	n = 7
1.1	42, 2.65	37, 2.57
	64.74, 84.69	52.13, 67.97
1.2	23, 2.52	19, 2.43
	21.35, 27.11	15.75, 19.66
1.5	8, 2.28	7, 2.22
	4.18, 4.44	3.02, 2.89
2.0	4, 2.11	3, 2.03
	1.72, 1.27	1.38, 0.82
2.5	3, 2.05	3, 2.03
	1.29, 0.67	1.12, 0.38
τ	n = 10	n=15
1.1	35, 2.52	31, 2.48
	41.27, 53.44	31.15, 39.93
1.2	16, 2.37	13, 2.32
	11.43, 13.91	7.84, 9.14
1.5	5, 2.14	4, 2.09
	2.22, 1.91	1.63, 1.13
2.0	3, 2.03	2, 1.94
	1.17, 0.47	1.05, 0.24
2.5	2, 1.94	2, 1.94
	1.04, 0.20	1.01, 0.07

Note that for the traditional side-sensitive synthetic γ chart without the VSI feature, W is not one of the charting parameters as the charting regions are not separated into warning and central regions. Thus, the same sampling interval, i.e. d=1, is always adopted in Table 7, unlike the VSI side-sensitive synthetic γ chart which varies the sampling interval between d_1 and d_2 . Hence, Table 7 is not separated into different d_1 and d_2 values.

By comparing Tables 3 and 7, the VSI side-sensitive synthetic γ chart gives lower ATS1 and SDTS1 compared to its fixed sampling interval counterpart, which indicates that the VSI feature enhances the detection capability of the side-sensitive synthetic γ chart. For example, for $\gamma_0 = 0.05$, n = 5, $\tau = 1.1$ and $(d_1, d_2) = (0.1, 1.5)$, the ATS1 and

*SDTS*1 of the VSI side-sensitive synthetic γ chart are 60.88 and 80.96, respectively, while that of its counterpart without the VSI feature are 64.74 and 84.69, respectively. For the choice of charting parameters, they (L,K) are the same for both charts.

IV. ILLUSTRATIVE EXAMPLE

This section considers an actual example from Castagliola *et al.* (2013), where the weight of scrap zinc alloy to be removed between the moulding process and the continuous plating surface treatment is being monitored during the manufacturing of zinc alloy parts for the sanitary sector. Excessive scrap is a result of uncontrolled item solidification resulting from a change in the injection pressure of the zinc alloy into the die (Castagliola *et al.*, 2013).

Due to the constant proportionality between σ and μ , the γ will be monitored. From 30 in-control samples of size n=5, Castagliola et al. (2013) has estimated γ_0 as 0.01. From Castagliola et al. (2013), a shift of $\tau = 1.2$ is an indication of uncontrolled item solidification and it is important for the manufacturer to be alerted of this condition. Furthermore, the manufacturer would prefer $(d_1, d_2) = (0.3 \text{ hours}, 1.7 \text{ hours})$ (Castagliola *et al.*, 2013). Hence, by using the methodology presented in Section II, the optimal parameters (L, W, K) = (23, 0.69, 2.52) that give $(ATS_1, SDTS_1) = (18.57, 24.82)$ are obtained, and the control limits are calculated as LCL = 0.00081, LWL = 0.0071, CL = 0.0094, UWL = 0.012 and UCL = 0.018.

The charting parameters in the preceding paragraph will be adopted to monitor 20 samples of size 5 following the occurrence of an out-of-control assignable cause. The first 10 samples are out-of-control, while after the 10th sample, efforts are taken to remove the assignable cause. Table 8 shows the $\hat{\gamma}$ of these 20 samples, together with the cumulative time until the sample is collected. Note that for $0.0071 < \hat{\gamma}_i < 0.012$, $d_{i+1} = 1.7$, while for other values of $\hat{\gamma}_i$, $d_{i+1} = 0.3$. The sample is non-conforming when $\hat{\gamma}_i > 0.018$ or $\hat{\gamma}_i < 0.00081$. The values in-bold are the non-conforming samples. For a graphical illustration, Figure 3 shows the $\hat{\gamma}$ plotted against the warning and control limits.

Table 8. Cumulative time and $\hat{\gamma}$ of 20 samples

i	Cumulative	$\hat{\gamma}_i$
	time (in hours)	
1	0.3	0.0053
2	0.6	0.0025
3	0.9	0.0036
4	1.2	0.0057
5	1.5	0.020
6	1.8	0.014
7	2.1	0.017
8	2.4	0.023
9	2.7	0.029
10	3.0	0.020
11	3.3	0.018
12	3.6	0.015
13	3.9	0.015
14	4.2	0.014
15	4.5	0.011
16	6.2	0.010
17	7.9	0.011
18	9.6	0.011
19	11.3	0.0038
20	11.6	0.0106

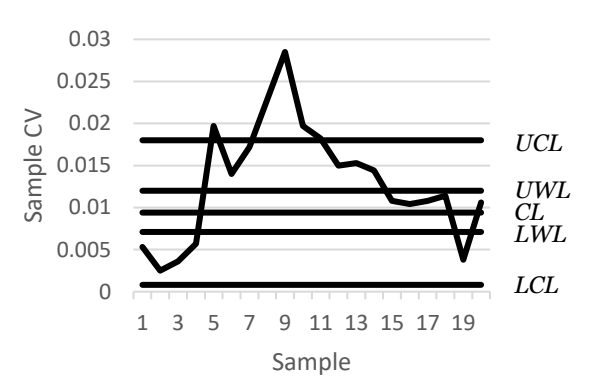


Figure 3. The VSI side-sensitive synthetic γ chart monitoring the weight of scrap zinc alloy

From Table 8 and Figure 3, the first non-conforming sample was observed at sample 5, 1.5 hours after process monitoring has started. This gives a CRL_1 of 5, which is less than the L of 23. Hence, an out-of-control signal is generated. Subsequently, samples 8 to 11 are also non-conforming, with CRL less than L. Hence, out-of-control signals are also generated. Out-of-control signals are produced 1.5, 2.4, 2.7, 3.0 and 3.3 hours after the commencement of process monitoring, showing quite frequent out-of-control signals.

After sample 11, the process starts to go back to an in-control condition, where d_2 is adopted for samples 16 to 19.

For the traditional side-sensitive synthetic γ chart, the same optimal (L,K) as the VSI side-sensitive synthetic γ chart is obtained, i.e. the same LCL=0.00081, CL=0.0094 and UCL=0.018 is adopted, with the exception that the chart does not show a warning region. Figure 4 shows a graphical representation of the side-sensitive synthetic γ chart.

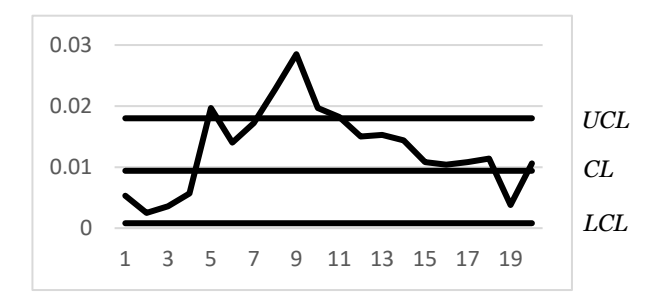


Figure 4. The side-sensitive synthetic γ chart monitoring the weight of scrap zinc alloy

From Figure 4, the same samples as the VSI side-sensitive synthetic γ chart, i.e. samples 5, 8, 9, 10 and 11, are detected as non-conforming samples. Since the CRL is less than L for all these non-conforming samples, out-of-control signals are generated. However, all these samples are taken at regular intervals of 1 hour, hence the traditional side-sensitive synthetic γ chart produces out-of-control signals only after 5, 8, 9, 10 and 11 hours from the commencement of process monitoring, unlike the VSI side-sensitive synthetic γ chart

which produces out-of-control signals 1.5, 2.4, 2.7, 3.0 and 3.3 hours after commencement. This shows that incorporating the VSI feature increases the speed of detection. Furthermore, when the process is in-control, the sampling is more frequent than necessary for the traditional side-sensitive synthetic γ chart. Unlike the VSI side-sensitive synthetic γ chart which adopts d_2 = 1.7 hours for samples 16 to 19 (note that samples 16 to 19 comes from an in-control process), the side-sensitive synthetic γ chart still carries out sampling at regular intervals of 1 hour, demonstrating that the sampling is carried out more frequent than necessary.

V. CONCLUSION

The VSI side-sensitive synthetic γ chart is proposed, and its optimal charting parameters are illustrated through several numerical examples. From the numerical examples, larger τ and n result in better performance, at the same time it results in the choice of smaller L and K. Furthermore, the numerical examples show that smaller W are adopted for larger gaps between d_1 and d_2 . From the performance comparison, the proposed chart outperforms its counterpart without the VSI feature. Implementation on an illustrative example shows that the proposed chart can quickly detect assignable cause(s), while showing less frequent sampling when in-control. Hence, it is advantageous to include the VSI feature for the sidesensitive synthetic γ chart. From the advantage of including the VSI feature, future research could explore the chart with variable sample size, as well as variable warning and control limits. The multivariate case could also be explored.

VI. REFERENCES

Amdouni, A, Castagliola, P, Taleb, H & Celano, G 2017, 'A variable sampling interval Shewhart control chart for monitoring the coefficient of variation in short production runs', International Journal of Production Research, vol. 55, no. 19, pp. 5521-5536.

Adsiz, S & Aytacoglu, B 2024, 'Tukey-EWMA control chart with variable sampling intervals for process monitoring', Quality Engineering, vol. 36, no. 2, pp. 249-272.

Ayyoub, HN, Khoo, MBC, Saha, S & Lee, MH 2022, 'Variable sampling interval EWMA chart for multivariate coefficient of variation', Communications in Statistics – Theory and Methods, vol. 51, no. 14, pp. 4617-4637.

Bai, Y, Chiang, JY, Liu, W & Mou, Z 2024, 'An enhanced EWMA chart with variable sampling interval scheme for monitoring the exponential process with estimated parameter', Scientific Reports, vol. 14, 7958.

- Calzada, ME & Scariano, SM 2013, 'A synthetic control chart for the coefficient of variation', Journal of Statistical Computation and Simulation, vol. 83, no. 5, pp. 853-867.
- Castagliola, P, Celano, G & Psarakis, S 2011, 'Monitoring the coefficient of variation using EWMA charts', Journal of Quality Technology, vol. 43, no. 3, pp. 249-265.
- Castagliola, P, Achouri, A, Taleb, H, Celano, G & Psarakis, S 2013, 'Monitoring the coefficient of variation using a variable sampling interval control chart', Quality and Reliability Engineering International, vol. 29, no. 8, pp. 1135-1149.
- Celano, G & Castagliola, P 2016, 'A synthetic control chart for monitoring the ratio of two normal variables', Quality and Reliability Engineering International, vol. 32, no. 2, pp. 681-696.
- Hu, XL, Zhang, SY, Xie, FP & Song, Z 2024, 'Triple exponentially weighted moving average control charts without or with variable sampling interval for monitoring the coefficient of variation', Journal of Statistical Simulation and Computation, vol. 94, no. 3, pp. 536-570.
- Nguyen, QT, Tran, KP, Heuchenne, HL, Nguyen, TH & Nguyen, HD 2019, 'Variable sampling interval Shewhart control charts for monitoring the multivariate coefficient of variation in the presence of measurement errors', Applied Stochastic Models in Business and Industry, vol. 35, no. 5, pp. 1253-1268.
- Nguyen, QT, Giner-Bosch, V, Tran, KD, Heuchenne & Tran, KP 2021, 'One-sided variable sampling interval EWMA control charts for monitoring the multivariate coefficient of variation in the presence of measurement errors', The International Journal of Advanced Manufacturing Technology, vol. 115, pp. 1821-1851.
- Rajmanya, SV, Ghute, VB 2014, 'A synthetic control chart for monitoring process variability', Quality and Reliability Engineering International, vol. 30, no. 8, pp. 1301-1309.
- Reh, W & Scheffler, B 1996, 'Significance tests and confidence intervals for coefficients of variation', Computational Statistics & Data Analysis, vol. 22, no. 4, pp. 449-452.

- Saccucci, MS, Amin, RW & Lucas JM 1992, 'Exponentially weighted moving average control scheme with variable sampling intervals', Communications in Statistics-Simulation and Computation, vol. 21, no. 3, pp. 627-657.
- Tran, PH & Heuchenne, C 2021, 'Monitoring the coefficient of variation using variable sampling interval CUSUM control charts', Journal of Statistical Computation and Simulation, vol. 91, no. 3, pp. 501-521.
- Wu, Z & Spedding, TA 2000, 'A synthetic control chart for detecting small shifts in the process mean', Journal of Quality Technology, vol. 32, no. 1, pp. 32-38.
- Wu, Z & Spedding, TA 2001, 'A synthetic chart for detecting fraction nonconforming increases', Journal of Quality Technology, vol. 33, no. 1, pp. 104-111.
- Xie, FP, Castagliola, P, Li, Z, Sun, JS & Hu, XL 2022, 'One-sided adaptive truncated exponentially weighted moving average \bar{X} schemes for detecting process mean shifts', Quality Technology & Quantitative Management, vol. 19, no. 5, pp. 533-561.
- Yeong, WC, Khoo, MBC, Tham, LK, Teoh, WL, Rahim, MA 2017, 'Monitoring the coefficient of variation using a variable sampling interval EWMA chart', Journal of Quality Technology, vol. 49, no. 4, pp. 380-401.
- Yeong, WC, Lee, PY, Lim, SL, Khaw, KW & Khoo, MBC 2021, 'A side-sensitive synthetic coefficient of variation chart', Quality and Reliability Engineering International, vol. 37, no. 5, pp. 2014-2033.
- Yeong, WC, Lim, SL, Khoo, MBC, Ng, PS & Chong, ZL 2022, 'A variable sampling interval run sum chart for the coefficient of variation', Journal of Statistical Computation and Simulation, vol. 92, no. 15, pp. 3150-3166.
- Yeong, WC, Tan, YY, Lim, SL, Khaw, KW & Khoo, MBC 2024, 'Variable sample size and sampling interval (VSSI) and variable parameters (VP) run sum charts for the coefficient of variation', Quality Technology & Quantitative Management, vol. 21, no. 2, pp. 177-199.